

# ROBOT SELF-LOCALIZATION

## *Using Omni-directional Histogram Correlation*

William F. Wood, Arthur T. Bradley, Samuel A. Miller and Nathanael A. Miller  
*NASA Langley Research Center, 5 N. Dryden St., Hampton, VA 23681 U.S.A.*  
*william.f.wood@nasa.gov, arthur.t.bradley@nasa.gov*

Keywords: Self-localization, Omni-directional, Histograms.

Abstract: In this paper, we describe a robot self-localization algorithm that uses statistical measures to determine color space histograms correlations. The approach has been shown to work well in environments where spatial nodes have unique visual characteristics, including rooms, hallways, and outdoor locations. A full color omni-directional camera was used to capture images for this localization work. Images were processed using user-created algorithms in National Instrument's LabView software development environment.

## 1 INTRODUCTION

The ability for a robot to locate itself in a local or global frame gives a unique positional awareness that leads to better navigational choices, optimized path planning, and topological mapping. One type of robot localization is to rely on external sources (e.g. GPS, internet access, human input, etc.) to inform the robot of its relative and perhaps absolute position. For remote missions however, with areas that are inaccessible, previously unexplored, have lengthy control delays, or have no support structure available, the robot must perform self-localization. Our goal in investigating robot self-localization was to mimic a human's ability to determine his/her location – generally done using a combination of sensory inputs and historical references. Topological localization of this type requires that a robot learn its environment, creating its own database of unique locations as well as a nodal map showing how the locations are interconnected.

Our work builds on previous research in which an omni-directional camera was used for histogram correlation (Ulrich, 2000) (Abe, 1999). Our research selects the best of three statistical measures with an averaging process to better perform scene recognition. The averaged approach leads to different scoring and voting systems, and requires fewer images per node to achieve acceptable results.

The method of histogram correlation is first introduced. Existing as well as new algorithms are then discussed using both equations and a flow

chart. And finally the results of correlating for several locations are examined.

## 2 HISTOGRAMS

There are many possible methods for self-localization, including approaches based on colors, sound, infrared images, range signatures, and object recognition. We used color histogram matching, because it was believed to closely emulate a human's ability to perform area recognition by broad color differentiation. The approach uses four primary color spaces, each with three 8-bit color bands: Red, Green and Blue (RGB); Hue, Saturation and Luminosity (HSL); Hue, Saturation and Value (HSV); and Hue, Saturation and Intensity (HSI), as well as normalized versions of those spaces. Normalized color spaces are created by normalizing the individual color bands with the total color value. For example, normalized RGB would be calculated using (1).

$$N_x = \frac{X}{R + G + B} \quad (1)$$

Where  $N_x$  is the normalized value and  $X$  can be R, G, or B.

Processing full color images require a great deal of processing capability and memory. Therefore all images were converted into color histograms before correlation. Histograms are typically two-dimensional representations of the distribution of

colors in an image. One axis of the histogram corresponds to the color bins (e.g. shades of red – dark to light), and the other axis corresponds to the number of pixels in the image that fall in this color bin. It serves as a statistical description of the occurrence of different color regions and is often used by photographers to prevent over/under exposure.

Consider an image captured using the RGB color space. Three separate histograms are created, one for each color band (R, G, B). The histogram for the R band is shown in Figure 1. For this particular histogram, we can see that the single red line represents the red 8-bit color band. The horizontal axis value of 0 translates to the zero brightness bin (usually indicating a black color). Likewise, the horizontal value of 255 indicates the maximum brightness bin. In this case, the red peak occurs at a bin value of ~97. Also note that a second peak occurs at the value of 255 indicating that there is some white content to the image.

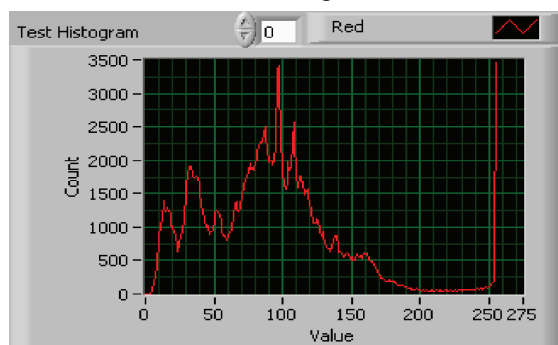


Figure 1: Sample histogram of R band.

The obvious advantage of converting images to a descriptive histogram is the significant file size reduction. A full color 16-bit resolution 640 x 480 image requires about 4.92 Mb of memory (assuming uncompressed data). Whereas the same image described as three histograms require only 6.1 kb (8-bit count x 255 bins x 3 bands). Reduced file sizes make both data storage and image correlation much less intensive. Furthermore, the histogram size is independent of the image size, making algorithms easily transportable between systems.

The disadvantage of histograms is that they are representations of color only, and have no information about object shape or texture. For that reason, completely different images can theoretically have identical histograms as seen in Figure 2.

In practice however, we have found that the histogram of a complex space (e.g. a cluttered room or parking lot) is quite unique and can be used for self localization.

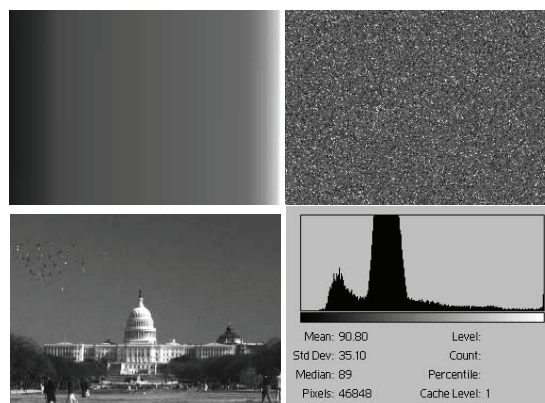


Figure 2: Three images share same histogram (bottom right).

### 3 IMAGE CAPTURE

For this investigation, we used a camera system with an omni-directional field of view (FOV). Omni-directional images are insensitive to rotation and work well when combined with histograms, which are insensitive to translation and inclination. It also allows for a single image to capture an entire location. As shown in Figure 3, the omni-directional FOV was achieved using a CCD VGA camera and a parabolic mirror.

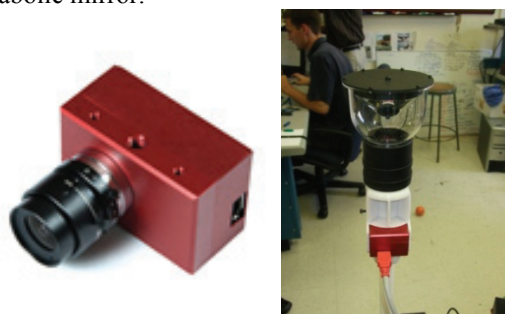


Figure 3: Videre Designs CCD camera and SOIOS omni-directional mirror.

One shortcoming of our camera was that it does not have either auto-brightness or auto-focus controls. The brightness issue was remedied by using an auto-brightness control algorithm. However, we were forced to use a manual single fixed focal length for the experiment. In a practical system, auto focus would be a beneficial for reliable localization.

LabVIEW 8.5 by National Instruments was used for analysis and to communicate with the camera via an IEEE 1394 interface. LabVIEW provides an object-oriented programming environment to easily

convert images to histograms and perform statistical correlation.

Images taken by the omni-directional camera appear as “donut-shaped,” with a dead space in the center corresponding to the parabolic reflection of our lens and mounting assembly. Figure 4 shows a sample image from our camera system.



Figure 4: Sample omni-directional image.

The black rectangular border (caused by the CCD shape) and the vertex dead space were removed by a masking algorithm, preventing them from being used in the image-to-histogram conversions.

## 4 STATISTICAL HISTOGRAM-MATCHING

The concept on statistical histogram matching was reported by a group of researchers at Carnegie Mellon University (Ulrich, 2000). Their work uses three statistical measures to correlate histograms:  $\chi^2$ , Jeffrey divergence (JD), and Kolmogorov-Smirnov (KS). We used the same statistical measures in our research. They are briefly discussed below (Papoulis, 2002).

### 4.1 $\chi^2$ Statistics

The  $\chi^2$  method is a bin-by-bin histogram distance difference calculation.  $H$  and  $K$  are sets of color histograms from two comparing images. They can be from any color space: RGB, HSV, HSL or HSI. However to correlate them, both histogram sets must describe the same color space. Let elements  $h_{ij}$  and  $k_{ij}$  describe the individual entries of  $H$  and  $K$ , where  $i$  represents the bin number and ranges from 0 to 255 and  $j$  represents the particular color band (e.g. R, G, or B if RGB space is being used).

By this definition, there are three sets of  $h_i$  and  $k_i$  pairs. For example in RGB case, there are  $h_{iR}, k_{iR}, h_{iG}, k_{iG}$  and  $h_{iB}, k_{iB}$ . The distance between the two histograms is defined by (2) and is a normalized measure of how well the two histograms correlate across all three color bands. Perfect correlation would yield a distance of zero.

$$d(H, K) = \sum_{i,j} \frac{(h_{ij} - k_{ij})^2}{k_{ij}} \quad (2)$$

### 4.2 Jeffrey Divergence (JD) Statistics

The Jeffrey Divergence method is also a bin-by-bin histogram distance difference calculation. Using the same notation as defined with  $\chi^2$ , the distance between two histograms is given by (3).

$$d(H, K) = \sum_{i,j} h_{ij} \cdot \log_2 \left( \frac{2 \cdot h_{ij}}{h_{ij} + k_{ij}} \right) + \sum_{i,j} k_{ij} \cdot \log_2 \left( \frac{2 \cdot k_{ij}}{h_{ij} + k_{ij}} \right) \quad (3)$$

Once again the distance between two identical images would be zero.

### 4.3 Kolmogorov-Smirnov (KS) Statistics

The Kolmogorov-Smirnov method is a third statistical measure, one that looks for the greatest difference between bins. The distance is then given by (4).

$$d(H, K) = \max |h_{ij} - k_{ij}| \quad (4)$$

## 5 IMAGE CORRELATION

To perform self-localization, the robotic system must first capture one or more training images for each location. This can be done a priori in a controlled manner, or dynamically as the robot first maps an unexplored area. The training images (stored as histograms) are kept in a database and used to correlate against real-time images (also converted to histograms), helping the robot to determine its location.

When performing self-localization, the robot correlates one or more real-time images (perhaps taken from different vantage points in a location) with the training images for every known location

(a.k.a. nodes). In the most favorable case, the robot would have numerous training images for every location to help with correlation accuracy.

The process of correlating an image is illustrated as a flow diagram in Figure 5. The test image is first converted to a histogram of the appropriate color space. A statistical method is then selected. Next, the distance between the test image and each training image of a given node is calculated. The distances between the test image and all training images for that node are then averaged. The process is repeated across all training nodes, with each training node yielding a distance result. If additional test images are available, the correlation process is repeated, with the results averaged with those from the first test image correlation.

Mathematically, the formulas to perform location recognition are best presented in operational stages. The distance between a single test image and a single training image is calculated by one of the three statistical distance equations (2), (3), (4). Additional test-to-training distances are calculated and combined for every training image in a node. The combined distance between a test image and all images in a training node is defined by the following.

$$D_x(H, K) = \sum_n \frac{d_x(H, K)}{3n} \quad (5)$$

Where  $x$  is the training node number,  $n$  is the number of training images, and 3 averages across the three color bands. The result is an averaged distance indicating how well a single test image correlates to multiple training images from node  $x$ . This process is repeated across all nodes, yielding a set of distance values between the image and each training node.

If more than one test image is available, the process is repeated with the results again averaged. In this case, the result is a set of total distances between a group of test images and each of the training nodes.

$$D_{tot-x}(H, K) = \sum_m \frac{D_x(H, K)}{m} \quad (6)$$

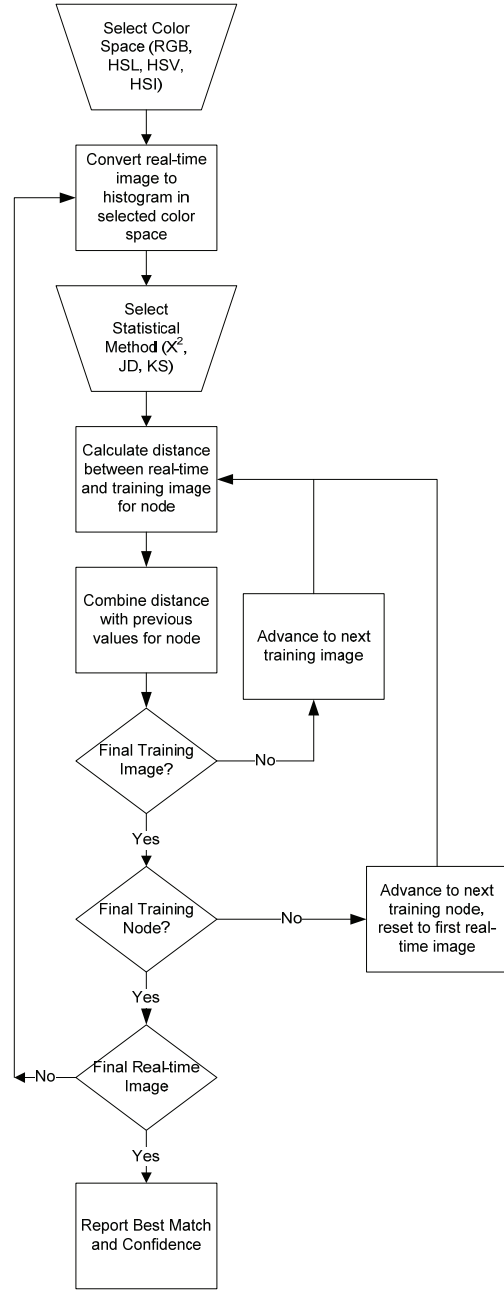


Figure 5: Correlation process.

Where  $m$  is the number of test images and  $x$  is the training node.

For each statistical method, the single formula representations for the total distance between a set of test images and a set of training images from a training node are given in the final section by (8), (9), and (10).

## 6 CONFIDENCE DETERMINATION

Each test image is ultimately identified as a particular training location based on which one it best matched. If multiple test images are available, then a correlation confidence is calculated.

$$c = \frac{\# \text{ of images agreeing on location}}{\# \text{ of test images}} \quad (7)$$

For example if there are 10 test images, and 9 of them agree on the location (based on correlation results), then the confidence is calculated as 90%.

The selection process can be made more robust by performing the distance calculations using all three statistical methods and then selecting the location based on the method that yields the highest level of confidence. Likewise, calculations can be made for more than one color space (RGB, HSL, etc.) and the best results selected.

## 7 RESULTS

The test set up was consistent for all images, with fixed camera height and focus. Also, the nodes remained generally unchanged without the presence of numerous people or other dynamic objects. The omni-directional lens removed the need to consider camera orientation. Finally, the RoboticVision program performed auto-brightness to eliminate significant light variations.

Testing consisted of first capturing 15 training images for 10 different locations (a.k.a. nodes). Obviously, the greater the number of nodes, the more difficult the final correlation. Likewise, the greater the number of training images, the easier the correlation. Training nodes consisted of 6 rooms, 1 hallway, and 3 outdoor locations.

The robot then maneuvered to each location of interest collecting 15 test images before performing correlation. Fewer training and test images are certainly possible, but the increased number helped to make the correlation more robust. Test and train images were also taken on the same day to help reduce dynamic changes (e.g. light, objects moved, etc.) that might have occurred to the locations. We realize this is an oversimplification, but the goal was to prove the initial theory before introducing additional uncertainties.

Overall the algorithm did a good job of correctly identifying the robot's location. For example, Figure

6 and Figure 7 show a training and test image for Room 215. The correlation results are given in Table 1. Additional nodes are given in Tables 2 - 7.

### Test Room 215 (Conference Room)

Non-normalized RGB was the only color space that failed to correctly identify Room 215. However, all other approaches and color spaces selected the correct room with a minimum of 73.3% confidence.

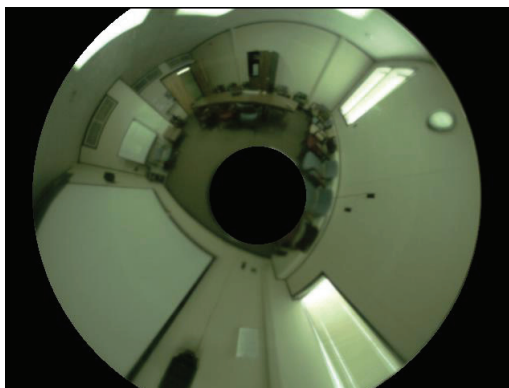


Figure 6: Training image for Room 215.

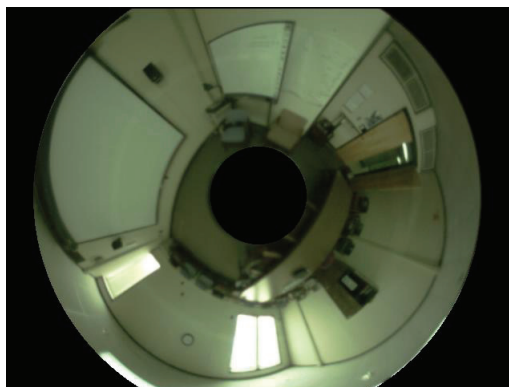


Figure 7: Test image for Room 215.

Table 1: Correlation results for Room 215.

| Color Space    | Node Selected | % Confidence |
|----------------|---------------|--------------|
| RGB            | Room 222      | 73.3         |
| Normalized RGB | Room 215      | 80           |
| HSL            | Room 215      | 100          |
| Normalized HSL | Room 215      | 73.3         |
| HSV            | Room 215      | 100          |
| Normalized HSV | Room 215      | 80           |
| HSI            | Room 215      | 100          |
| Normalized HSI | Room 215      | 73.3         |

The results from Room 215 illustrate the benefits of normalizing the color spaces prior to correlation. In particular, the RGB color space correlation is improved when normalization of histogram data is done.

Room 222 (Conference Room)

Room 222 was correctly chosen using all color spaces with a high degree of confidence.



Figure 8: Test image for Room 222.

Table 2: Correlation results for Room 222.

| Color Space    | Node Selected | % Confidence |
|----------------|---------------|--------------|
| RGB            | Room 222      | 100          |
| Normalized RGB | Room 222      | 93.3         |
| HSL            | Room 222      | 100          |
| Normalized HSL | Room 222      | 100          |
| HSV            | Room 222      | 100          |
| Normalized HSV | Room 222      | 86.7         |
| HSI            | Room 222      | 100          |
| Normalized HSI | Room 222      | 93.3         |

Room 226A (Small Meeting Room)

Room 226A was correctly chosen using 7 of the 8 color spaces. Again non-normalized RGB was the single failure.



Figure 9: Test image for Room 226A.

Table 3: Correlation results for Room 226A.

| Color Space    | Node Selected | % Confidence |
|----------------|---------------|--------------|
| RGB            | Room 218      | 60           |
| Normalized RGB | Room 226A     | 66.7         |
| HSL            | Room 226A     | 86.7         |
| Normalized HSL | Room 226A     | 73.3         |
| HSV            | Room 226A     | 80           |
| Normalized HSV | Room 226A     | 80           |
| HIS            | Room 226A     | 80           |
| Normalized HIS | Room 226A     | 86.7         |

Room 246 (Large Conference Room)

Room 246 was correctly chosen using all color spaces with a high degree of confidence.

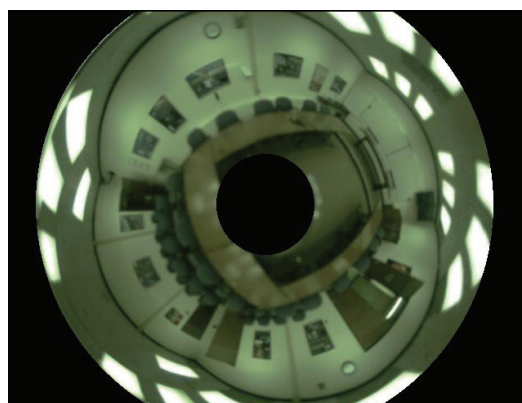


Figure 10: Test image for Room 246.

Table 4: Correlation results for Room 246.

| Color Space    | Node Selected | % Confidence |
|----------------|---------------|--------------|
| RGB            | Room 246      | 86.7         |
| Normalized RGB | Room 246      | 86.7         |
| HSL            | Room 246      | 93.3         |
| Normalized HSL | Room 246      | 100          |
| HSV            | Room 246      | 93.3         |
| Normalized HSV | Room 246      | 100          |
| HIS            | Room 246      | 93.3         |
| Normalized HIS | Room 246      | 100          |

Sidewalk

The Sidewalk was identified correctly with 86.7% confidence due to the significant color differences.

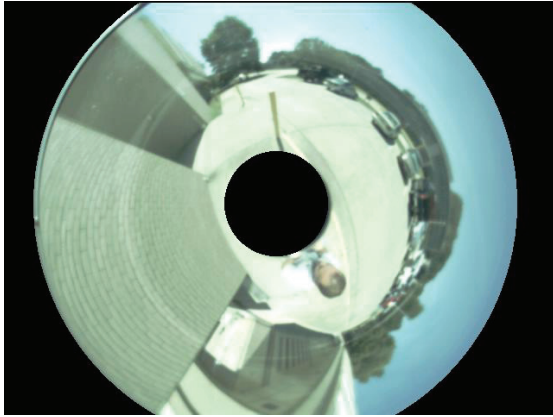


Figure 11: Test image for Sidewalk.

Table 5: Correlation results for Front Sidewalk.

| Color Space    | Node Selected | % Confidence |
|----------------|---------------|--------------|
| RGB            | Sidewalk      | 86.7         |
| Normalized RGB | Sidewalk      | 86.7         |
| HSL            | Sidewalk      | 93.3         |
| Normalized HSL | Sidewalk      | 100          |
| HSV            | Sidewalk      | 93.3         |
| Normalized HSV | Sidewalk      | 100          |
| HIS            | Sidewalk      | 93.3         |
| Normalized HIS | Sidewalk      | 100          |

#### Front Parking Lot

The Front Parking Lot was also easily identified because of the distinct outdoor color signatures.



Figure 12: Test image for Front Parking Lot.

Table 6: Correlation results for Front Parking Lot.

| Color Space    | Node Selected | % Confidence |
|----------------|---------------|--------------|
| RGB            | F. Parking    | 100          |
| Normalized RGB | F. Parking    | 100          |
| HSL            | F. Parking    | 100          |
| Normalized HSL | F. Parking    | 93.3         |
| HSV            | F. Parking    | 100          |
| Normalized HSV | F. Parking    | 100          |
| HIS            | F. Parking    | 100          |
| Normalized HIS | F. Parking    | 100          |

#### Rear Parking Lot

Once again, the Rear Parking Lot was correctly identified with nearly 100% confidence.

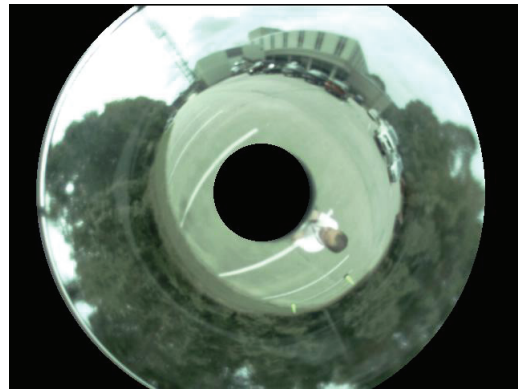


Figure 13: Test image for Rear Parking Lot.

Table 7: Correlation results for Front Parking Lot.

| Color Space    | Node Selected | % Confidence |
|----------------|---------------|--------------|
| RGB            | R. Parking    | 100          |
| Normalized RGB | R. Parking    | 100          |
| HSL            | R. Parking    | 100          |
| Normalized HSL | R. Parking    | 93.3         |
| HSV            | R. Parking    | 100          |
| Normalized HSV | R. Parking    | 100          |
| HIS            | R. Parking    | 100          |
| Normalized HIS | R. Parking    | 100          |

## 8 SUMMARY

It was demonstrated that color histograms can be used to perform self-localization, both indoors and outdoors. Three statistical measures were used to calculate the distance between training images and test images. Correlation results from multiple test and training images across different color spaces

were combined to create a robust correlation methodology.

Future work will include developing an autonomous topological mapping system based on the histogram self-localization algorithm. The mapping system will allow the robot to identify not only its current location but also its overall position in a larger map-based area. Once the robot's location is known, adjacency knowledge can be used to do zone filtering to greatly reduce search sizes.

This sensor-based self-localization could be of assistance in achieving efficient node-to-node navigation, path planning, and achieving other mission objectives.

## 9 CORRELATION EQUATIONS

$$\chi^2 \Rightarrow D_{tot}(H, K) = \sum_m \sum_n \sum_{i,j} \frac{(h_{ij} - k_{ij})^2}{3mnk_{ij}} \quad (8)$$

$$\begin{aligned} JD \Rightarrow D_{tot}(H, K) & \quad (9) \\ & = \sum_m \sum_n \frac{\left( \frac{\sum_{i,j} h_{ij} \cdot \log_2 \left( \frac{2h_{ij}}{h_{ij} + k_{ij}} \right) + \sum_{i,j} k_{ij} \cdot \log_2 \left( \frac{2k_{ij}}{h_{ij} + k_{ij}} \right)}{3mn} \right)}{3mn} \end{aligned}$$

$$KS \Rightarrow D_{tot}(H, K) = \sum_m \sum_n \sum_{i,j} \frac{\max|h_i - k_i|}{3mn} \quad (10)$$

## REFERENCES

- Ulrich, I., Nourbakhsh, I. "Appearance-Based Place Recognition for Topological Localization", *IEEE International Conference on Robotics and Automation*, April 2000, pp. 1023-1029.
- Papoulis, A., Pillai, S. Probability, *Random Variable and Stochastic Processes*, New York, NY: McGraw-Hill, 2002, ch. 8.
- Abe, Y., Shikano, M., Fukuda, T., Arai, F., and Tanaka, Y., "Vision Based Navigation System for Autonomous Mobile Robot with Global Matching", *IEEE International Conference on Robotics and Automation*, May 1999, pp. 1299-1304.
- Kuipers, B.J., "Modeling spatial knowledge," *Cognitive Science*, vol. 2, no. 2, pp. 129-153, 1978.